

Design and Analysis of A Robust Current Control Algorithm for Electric Motor Emulator[⊖]

Li Qi¹, Wang Dafang¹, Li Shuai², Zhang Yujin¹, Qin Yingkang¹

1. *Automotive Engineering College, Harbin Institute of Technology*
2. *China First Automobile Works (FAW) Group Co., Ltd.*

Abstract: A robust current control algorithm has been proposed to improve the dynamic performance of the Electric Motor Emulator (EME), which is used to fulfill the power-hardware-in-loop (PHIL) simulation for Electric Motor Control Unit (MCU) of Electric Vehicle. A disturbance observer (DO) is designed to compensate for the unmodeled dynamics and disturbances caused by parameter perturbations and control errors over the wide operating points, together with the feedforward controller and state feedback controller to form the proposed robust controller. The control goal of dynamic accuracy is derived based on the Singular Value analysis of the linearized motor model and the control goal of robust stability is guaranteed by checking the stability of the discretized motor model, open-loop EME system and closed-loop EME testing system by analysing the eigenvalues of the corresponding discrete system matrixes. Experimental results prove that the proposed control algorithm can provide improved robust dynamic current tracking performance compared with existing ones.

Key words: control algorithm, Electric Motor Emulator (EME), Power-Hardware-in-Loop (PHIL) simulation, Disturbance Observer (DO), stability analysis.

Introduction

Along with the development in computational and electronic device technology, power-hardware-in-loop (PHIL) simulation has been widely used in the fields of Electric Drives, Transportation and Power Grids^[1-16].

Accuracy and stability are the key concerns when performing the PHIL simulation. Various factors affecting the simulation accuracy and stability have been researched. The time delay is found to be the major influence on the stability of the PHIL system^[2], and a thorough assessment of the total loop delay in PHIL has been performed in^[3]. The importance of modeling and Control Algorithm, namely Interface Algorithm (IA), for accuracy and stability consideration of PHIL simulation is addressed by Wei Ren^[4]. Two types of Coupling Networks (CN) have been compared by Santiago^[1], and *LCL* type of CN seems to provide better dynamic performance compared with Link Inductor (LI) type of CN. Voltage type Ideal Transformer Model (ITM) IA together with closed-loop voltage control is adopted in emulating a Synchronous Generator (SG) in^[5], and it demonstrates that control parameters of proportional-integral (PI) and Feedforward (FF) controllers should be designed deliberately. Influence of parameters of a passive RL load on the stability has been analyzed based on the discrete-time (DT) model, which proves to predict the PHIL system stability more accurately compared with continuous-time

(CT) model^[6].

Electric Motor Emulator (EME) for testing Motor Control Unit (MCU) of Electric Vehicle is a special type of PHIL simulation device, which is being popular during the developing process of Electric Drive System^[7-10]. The simulation goal of EME is to perform electrically in the same manner as the real Electric Motor. The basic principle of the EME testing system is that (see Figure 1), the Real-Time Simulation Model of EME takes the three-phase voltage information of MCU as input and gives current setpoint values as output to the Current Control Algorithm, which calculates the command voltage of EME and sends it to the Power Amplifier to execute. The main specialties of the EME testing system can be listed as below, which brings a great challenge on achieving satisfied accuracy and stability performance.

- 1) MCU is an active DUT containing Current Controller, and the system tends to instability if the Current Controller of EME conflicts with the one of MCU^[8].
- 2) The CN cannot be omitted considering the high frequency PWM voltages of MCU and EME, and parameter perturbation of the CN exists, adding difficulties to the dynamic accuracy and stability analysis^[1].
- 3) Operating speed point of the Electric Drive motor varies considering the driving condition of a vehicle, resulting in changing dynamic behavior requirements at different operation points of the Motor Model^[7,9].

[⊖] This work was supported in part by the National Natural Science Foundation of China (52072098), in part by the Cultivation Program for Major Scientific Research Projects of HIT (ZDXMPY20180109) and in part by the Weihai Industrial Technology Research Institute special support funds of Shandong (202001PTXM05).

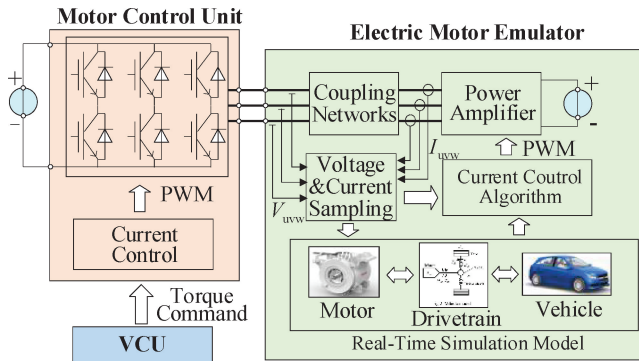


Figure 1 Block Diagram of EME testing system

So, it's of interest to design a stable EME system that can achieve high dynamic accuracy in a wide range of speed points and should be robust considering parameter perturbation and control disturbance. This paper mainly focuses on the design and analysis of the Current Control Algorithm, which plays a vital role on determining the performance of the EME system.

Various control methods have been used by researchers to promise an accurate and stable EME system, as well as other types of the PHIL system. An Open-Loop-VSI based PA is shown to be dynamically accurate if parameters of the passive LI load are accurately known^[6], and Open-Loop Control to emulate the Permanent Magnet Synchronous Motor (PMSM) is achieved based on the calculation of back electromotive voltage^[11], which is easy to be implemented but vulnerable to parameter deviations. PI controller is widely used in SISO system control, which is also easy to be carried out without the need of penetrating into the complex control theory. In [12], a DSP based ASM power simulator is realized by using PI controller, which may be the first one who tried to simulate a power motor. PI controller is also used in [1], which takes system bandwidth (BW) as a goal to derive the parameters of PI controller by abstracting the LI CN as a first-order transfer function. It's pointed in [8] that PI type current-loop BW of EME should be at least five times higher than the current-loop BW of MCU under test to promise a good accuracy and stability. Feedforward (FF) controller is added to PI controller in [5] and [13] to improve the dynamic performance of the PHIL simulation. Control methods based on Modern Control Theory can provide overall better performance by using the model information adequately. An inverse model based predictive control method is used to control the current flowing between the EME and DUT in [14] by building a discrete state-space (SS) Model of LCL type CN. Effectiveness of the state feedback control based on Optimal Control theory is demonstrated in [15] by emulating various types of electric load. Similar control method has also been used and tested in [16] to build a PHIL simulation system for load emulation. However, all these existing designs lacks the robustness of dynamic and stability by considering the modeling errors and wide operating points. A MIMO design method for high-speed EME with high robustness is proposed in [17], yet the

design is in the continuous-time domain, and the stability performance is not been taken into consideration.

A model-based Current Control Algorithm for EME system is proposed in this paper to improve the robustness of its dynamic accuracy and stability performance by taking parameter perturbations, control disturbances and the wide range of operating points into consideration, and the design is implemented in the discrete-time domain to make it more appropriate for digital applications.

The paper is organized as follows. Section II discusses the control goal of dynamic accuracy and stability, and the proposed current control algorithm is then demonstrated in Section III, with the performance analyzed in Section IV. Experiments that prove the effectiveness and improvement of the algorithm are shown in Section V, and conclusion is summarized in Section VI at the end.

1 Control Goal Analysis

The overall control structure of the EME testing system is shown in Figure 2 (abstracted from Figure 1) to clarify the control goal. Dynamics of the Vehicle Model and Drivetrain Model are often lying in the lower frequency range (no more than 20Hz), which are easy to emulate and therefore omitted during the control analysis. So, only the Motor Model (up to hundreds of Hertz) is considered here to analyze the control goal of accuracy and stability for clearance.

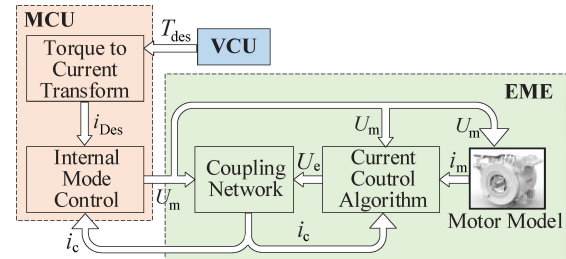


Figure 2 Control Structure of the EME testing system

1.1 Dynamic Accuracy Goal Analysis

PMSM is chosen as the target motor to emulate in this paper, whose mathematical representation (Motor Model in Figure 2) in rotor coordinates (the dq frame) is given by

$$\begin{cases} U_{dm}(t) = R_{sm}i_{dm}(t) + L_{dm}\frac{di_{dm}(t)}{dt} - L_{qm}\omega_e i_{qm}(t) \\ U_{qm}(t) = R_{sm}i_{qm}(t) + L_{qm}\frac{di_{qm}(t)}{dt} + L_{dm}\omega_e i_{dm}(t) + \omega_e \psi_{rm} \end{cases} \quad (1)$$

where U_{dm} and U_{qm} are the stator voltage from MCU; i_{dm} and i_{qm} are the stator currents, R_{sm} is the stator winding resistance; ω_e is the electrical rotor speed; L_{dm} and L_{qm} are the stator inductances, respectively. The term $\omega_e \psi_{rm}$ is the back EMF, which is embraced in $\xi_m = [0 \ \omega_e \psi_{rm}]^T$ as a slow-varying disturbance.

Equation (1) can be linearized in multi-input multi-output (MIMO) SS form as (2) by viewing $U_m = (U_{dm} \ U_{qm})^T$ as input and $i_m = (i_{dm} \ i_{qm})^T$ as the state variables

$$\frac{di_m}{dt} = A_m i_m + B_m U_m + \xi_m \quad (2)$$

Singular Values at each speed point of (2) can be obtained as Figure 3 by viewing ω_e as a time-varying parameter^[18], showing that the motor tends to be less damped with the increasing of ω_e owing to the cross-coupling effect between D and Q Axes. The control goal of dynamic accuracy is to mimic the frequency response of (2), i.e., to track the desired current i_m under different U_m input, and the main challenge is to emulate the resonance feature accurately as ω_e increases.

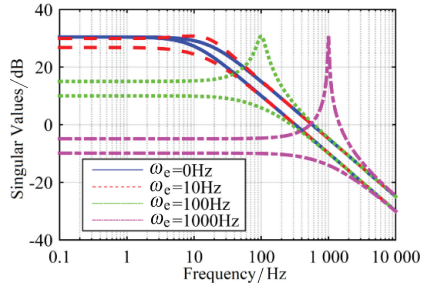


Figure 3 Singular Values of PMSM

($L_{dm} = 280\mu H$, $L_{qm} = 500\mu H$, $R_{sm} = 30m\Omega$)

1.2 Stability Goal Analysis

Compared with the augmented PHIL block diagram in [4] (see Figure 4a), the block diagram of EME testing system (see Figure 4b) is more complex. The closed-loop Current Control Algorithm exists in both EME and MCU, instability may occur if designed improperly. Besides, the system operates over a wide range of speed and parameter perturbations exist in CN. So, it's of great importance to clarify the stability goal and check the robustness before application in field. The control goal of stability of the EME testing system can be concluded as following steps: First, mathematical calculation of the discretized simulation motor model, as a subsystem, should be stable. Second, the EME system itself should be stable when the MCU operates at open-loop control mode (voltage mode). Last, the EME testing system considering the closed-loop current control mode of the MCU should be stable. The first stability goal involving motor model is discussed as follows while the other two goals will be shown in Section IV.

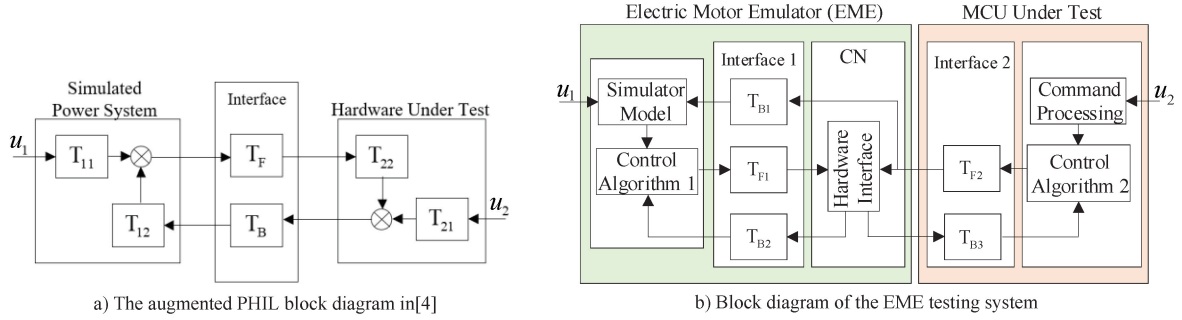


Figure 4 The block diagram of the augmented PHIL and EME test system

1.3 Stability of the Motor Model

Although both [9] and [10] point out that calculation interval of Motor Model should be small enough to ensure the accuracy, the relationship between the calculation interval and stability has not been addressed. The discretized representation of equation (2) can be derived as (3) by using Forward Euler method

$$i_m(k+1) = A_{mz} i_m(k) + B_{mz} U_m(k) \quad (3)$$

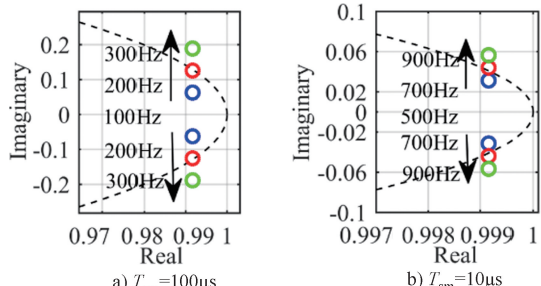
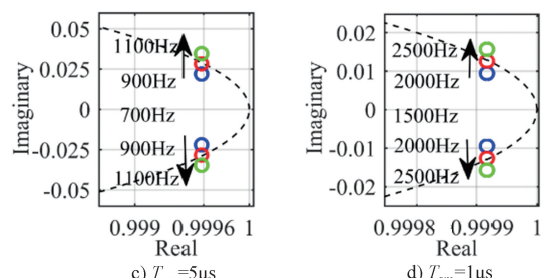


Figure 5 Eigenvalues of the discretized PMSM Model at different calculation intervals when ω_e varies

in which $A_{mz} = I + T_{sm} A_m$, $B_{mz} = T_{sm} B_m$, and T_{sm} is the calculation interval. The magnitude of all the eigenvalues of A_{mz} should be less than unity to promise the stability of the discretized motor model. It's shown from Figure 5 that, as T_{sm} is shortened, the upper speed-limit that the model can reach stably increases. The neutral stable points of the calculation interval T_{sm} versus the rotor speed ω_e are then plotted, and the first goal involving stability can thus be achieved only if the operating point of the Motor Model lies in the stable region in Figure 6.



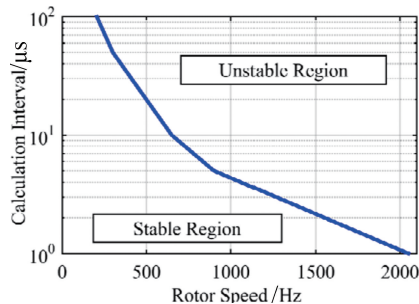


Figure 6 Stable and unstable regions of the discretized PMSM model

2 Proposed Current Control Algorithm

2.1 Modeling of the Coupling Networks (CN)

It can be seen from Figure 2 and Figure 4 that the CN (Hardware Interface) has great influence on the system performance, as both sides of the current controller take the current of the CN as a feedback and exert the PWM voltages on the CN to fulfill the closed-loop current control.

As shown in Figure 7, a three-phase Link Inductor (LI) CN, which is popular in PHIL simulation for its clear structure^[1,5,9], is used here, and its voltage equations can be described as follows according to [19]

$$\begin{cases} U_{dm} - U_{de} = L_c \frac{di_{dc}}{dt} + R_c i_{dc} - \omega_e L_c i_{qe} \\ U_{qm} - U_{qe} = L_c \frac{di_{qe}}{dt} + R_c i_{qe} + \omega_e L_c i_{dc} \end{cases} \quad (4)$$

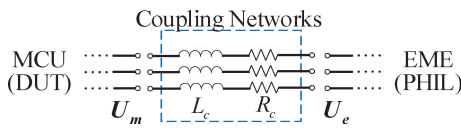
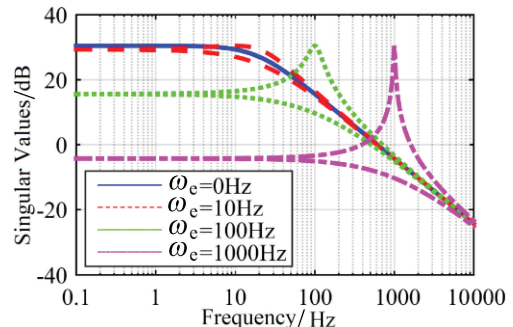


Figure 7 A three phase Link Inductor is implemented as the CN between the MCU and the EME

in which L_c and R_c stand for the inductance and resistance of the LI CN, and $\mathbf{U}_m = (U_{dm} \ U_{qm})^T$ and $\mathbf{U}_e = (U_{de} \ U_{qe})^T$ stand for the output voltages of MCU and EME respectively. MIMO SS form of equation (4) can be got by viewing CN currents $\mathbf{i}_c = (i_{dc} \ i_{qe})^T$ as state variables

$$d\mathbf{i}_c/dt = \mathbf{A}_c \mathbf{i}_c + \mathbf{B}_{c1} \mathbf{U}_m + \mathbf{B}_{c2} \mathbf{U}_e \quad (5)$$

in which $B_{c1} = -B_{c2}$, and the Singular Values at different speed of (5) are depicted in Figure 8 by taking \mathbf{i}_c as output and $(\mathbf{U}_m - \mathbf{U}_e)$ as input. It's of great benefit that Singular Values of the CN resemble with Motor models at different speed as shown in Figure 3. The control burden of EME can be eased if Singular Values of the Motor model and the CN match with each other absolutely, which is impossible considering the anisotropic characteristic ($L_d \neq L_q$) of the interior PMSM used in Electric Vehicles^[7] and the manufacturability of the CN.

Figure 8 Singular Values of LI CN with $L_c = 260 \mu\text{H}$, $R_c = 80 \text{ m}\Omega$

2.2 Proposed Control Algorithm

Considering that the dynamic BW requirement for the EME system increases as the speed increases (see Figure 3) and the system should be immune for parameter perturbations and voltage disturbances, a robust current control algorithm shown as Figure 9 is designed.

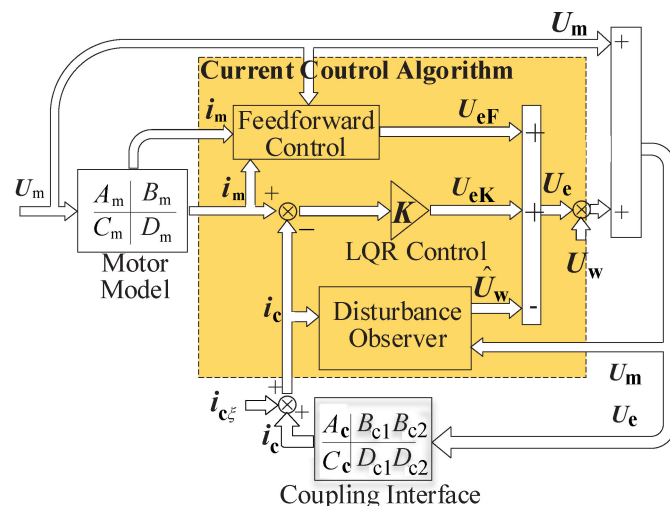


Figure 9 Structure of the proposed robust Current Control Algorithm

First, a Feedforward (FF) controller based on the target PMSM model and the LI CN model is built to guarantee the dynamic performance, and the optimal state feedback controller based on linear quadratic regulator (LQR) technique is used to promise a closed-loop MIMO system. Then, a Disturbance Observer is designed to compensate for the unmodeled dynamics and disturbances to improve the robustness of the control algorithm.

2.3 Feedforward and State Feedback Controller

Feedforward control method is widely used in PHIL simulation^[5,10]. The discretized form of a reference model of CN as (6) can be derived from (5) using Forward Euler principle. \mathbf{A}_{crz} , \mathbf{B}_{crz1} , and \mathbf{B}_{crz2} can be obtained based on the parameters of the reference CN model, i.e., L_{cr} and R_{cr}

$$\mathbf{i}_c(k+1) = \mathbf{A}_{crz} \mathbf{i}_c(k) + \mathbf{B}_{crz1} \mathbf{U}_m(k) + \mathbf{B}_{crz2} \mathbf{U}_e(k) \quad (6)$$

As the desired current of next calculation step can be easily got from (3), the discretized FF control law considering ξ_m can be obtained by assuming $i_e(k+1) = i_m(k+1)$

$$U_{eF}(k) = \mathbf{B}_{crz2}^+ [(\mathbf{A}_{mz} - \mathbf{A}_{crz}) i_m(k) + (\mathbf{B}_{mz} - \mathbf{B}_{crz1}) U_m(k) + \xi_m(k)] \quad (7)$$

in which $\mathbf{B}_{crz2}^+ = (\mathbf{B}_{crz2}^\top \mathbf{B}_{crz2})^{-1} \mathbf{B}_{crz2}^\top$ stands for the Penrose pseudo inverse matrix of \mathbf{B}_{crz2} .

As state feedback control is an effective way to form the MIMO plant into a closed loop system^[15,16], an optimal state feedback controller K is derived using the LQR by minimizing the performance index J in (8)

$$J = \frac{1}{2} \sum_{k=0}^n \{ [i_m(k) - i_e(k)]^\top \mathbf{Q} [i_m(k) - i_e(k)] + U_e^\top(k) \mathbf{R} U_e(k) \} \quad (8)$$

where \mathbf{Q} is a diagonal matrix that decides the weight of the control error and \mathbf{R} is the penalty that decides the weight of the output voltage of the EME. Attention should be paid for \mathbf{R}/\mathbf{Q} to promise the closed-loop performance of the system, i.e., dynamic accuracy, noise suppression and stability. Then the discrete control law of the state feedback controller can be obtained:

$$U_{ek}(k) = K [i_m(k) - i_e(k)] \quad (9)$$

2.4 Design of Disturbance Observer (DO)

Disturbance Observer (DO) based control and related methods are popular considering the promising effects on disturbance and uncertainty attenuation. The most notable advantage of the DO is that it eases the control conflicts of tracking versus noise rejection and nominal performance versus robustness by adding additional degree of control freedom^[20].

$$\begin{pmatrix} \hat{i}_e \\ \hat{U}_w \end{pmatrix} = \begin{pmatrix} \mathbf{A}_{cr} & \mathbf{B}_{cr2} \\ 0 & 0 \end{pmatrix} \begin{pmatrix} \hat{i}_e \\ \hat{U}_w \end{pmatrix} + \begin{pmatrix} \mathbf{B}_{cr1} \\ 0 \end{pmatrix}$$

and the discretized law for digital application is then derived

$$\begin{pmatrix} \hat{i}_e(k+1) \\ \hat{U}_w(k+1) \end{pmatrix} = \begin{pmatrix} \mathbf{A}_{crz} - \mathbf{L}_{1z} & \mathbf{B}_{cr2z} \\ -\mathbf{L}_{2z} & \mathbf{I} \end{pmatrix} \begin{pmatrix} \hat{i}_e(k) \\ \hat{U}_w(k) \end{pmatrix} + \begin{pmatrix} \mathbf{B}_{cr1z} & \mathbf{B}_{cr2z} & \mathbf{L}_{1z} \\ 0 & 0 & \mathbf{L}_{2z} \end{pmatrix} \begin{pmatrix} U_m(k) \\ U_e(k) \\ i_e(k) \end{pmatrix} \quad (15)$$

The final output voltage of the EME is shown as (17) by combining FF controller, State Feedback controller and DO

$$U_e(k) = U_{eF}(k) + U_{ek}(k) - \hat{U}_w(k) \quad (17)$$

It should be noted that the DO cannot be used independently, for the goal of the DO is to assimilate dynamics of the controlled CN with the reference model shown as (6) without knowing the tracking reference i_m . Therefore, the FF and the State Feedback Controller are necessary for the control structure to drive the Current Control Algorithm primarily.

$$\begin{pmatrix} i_m(k+1) \\ i_e(k+1) \\ \hat{i}_e(k+1) \\ \hat{U}_w(k+1) \end{pmatrix} = \underbrace{\begin{pmatrix} \mathbf{A}_{mz} & 0 & 0 \\ \mathbf{B}_{c2z} \mathbf{B}_{cr2z}^+ (\mathbf{A}_{mz} - \mathbf{A}_{crz}) + \mathbf{B}_{c2z} K & \mathbf{A}_{ez} - \mathbf{B}_{c2z} K & 0 \\ \mathbf{A}_{mz} - \mathbf{A}_{crz} + \mathbf{B}_{cr2z} K & \mathbf{A}_{crz} - \mathbf{L}_{1z} & 0 \\ 0 & \mathbf{L}_{2z} & I \end{pmatrix}}_{A_{EME}} \begin{pmatrix} i_m(k) \\ i_e(k) \\ \hat{i}_e(k) \\ \hat{U}_w(k) \end{pmatrix}$$

SS form of the CN is rewritten as (10) with \mathbf{B}_w representing the dynamic characteristics of the unmodeled disturbance d_w

$$di_e/dt = A_c i_e + B_{cl} U_m + B_{c2} U_e + B_w d_w \quad (10)$$

Assuming parameter errors exist between the real CN and the reference model ($L_c, R_c \neq L_{cr}, R_{cr}$), resulting in ΔA_{cr} , ΔB_{cr1} and ΔB_{cr2} for the SS matrix difference between real plant and reference model, shown as follows:

$$A_c = A_{cr} + \Delta A_{cr}, B_{cl} = B_{cr1} + \Delta B_{cr1}, B_{c2} = B_{cr2} + \Delta B_{cr2} \quad (11)$$

$$di_e/dt = A_{cr} i_e + B_{cr1} U_m + B_{cr2} U_e + \Delta A_{cr} i_e + \Delta B_{cr1} U_m + \Delta B_{cr2} U_e + B_w d_w \quad (12)$$

Terms involving model errors and disturbance above can be augmented into the disturbance U_w of the EME side by viewing

$$\Delta A_{cr} i_e + \Delta B_{cr1} U_m + \Delta B_{cr2} U_e + B_w d_w = B_{cr2} U_w \quad (13)$$

Then the final representation of the reference model used for the DO can be represented as follows:

$$di_e/dt = A_{cr} i_e + B_{cr1} U_m + B_{cr2} U_e + B_{cr2} U_w \quad (14)$$

The basic principle of the DO is to estimate the disturbances or uncertainties that are equivalent on the control output by fully employing the available information, and then compensate for them to conquer the adverse influence on system dynamics.

The observer shown as (15) is then designed based on the relationship between the input disturbance U_w and the measurable current of CN i_e established in (14), and $L = (L_1 \ L_2)^\top$ stands for the observer gain, which can be designed according to the desired control BW of dynamic accuracy to achieve a satisfied tracking performance between the estimated states $(\hat{i}_e \ \hat{U}_w)^\top$ and the real values of $(i_e \ U_w)^\top$

$$\begin{pmatrix} \hat{i}_e(k+1) \\ \hat{U}_w(k+1) \end{pmatrix} = \begin{pmatrix} \mathbf{U}_m \\ \mathbf{U}_e \end{pmatrix} + L \left[i_e - (I \ 0) \begin{pmatrix} \hat{i}_e \\ \hat{U}_w \end{pmatrix} \right]$$

as follows:

$$\begin{pmatrix} \hat{i}_e(k+1) \\ \hat{U}_w(k+1) \end{pmatrix} = \begin{pmatrix} \mathbf{B}_{cr1z} & \mathbf{B}_{cr2z} & \mathbf{L}_{1z} \\ 0 & 0 & \mathbf{L}_{2z} \end{pmatrix} \begin{pmatrix} U_m(k) \\ U_e(k) \\ i_e(k) \end{pmatrix} \quad (16)$$

3 Performance Analysis

Discrete State-Space (DSS) representation of the EME system, shown as (18), can be obtained by combining (3), (6), (7), (9), (16) and (17). Performance analysis of dynamic accuracy and stability can be carried out based on the derived DSS representation of system, which adopts the proposed current control algorithm stated above.

$$+ \begin{bmatrix} \mathbf{B}_{mz} \\ \mathbf{B}_{c1z} + \mathbf{B}_{c2z} \mathbf{B}_{cr2z}^+ (\mathbf{B}_{mz} - \mathbf{B}_{cr1z}) \\ \mathbf{B}_{mz} \\ 0 \end{bmatrix} \mathbf{U}_m(k) \quad (18)$$

3.1 Dynamic Performance Analysis

The transfer function perturbation (TFP) based error model is an effective way on assessing the emulation accuracy^[4,5], and the Singular Values of i_c/U_w (TFP of the EME system shown in Figure 9) are shown in Figure 10. It's shown in the Figure that although effects of disturbance U_w on i_c can be reduced with increasing Q index of the LQR control method (without DO), which means higher open-loop gain, the steady state error cannot be fully eliminated. As a contrast, the DO can fully wipe out the steady error (Singular Values tends to negative infinity at 0 Hz) by estimating the disturbance and/or the uncertainties and then compensating for them.

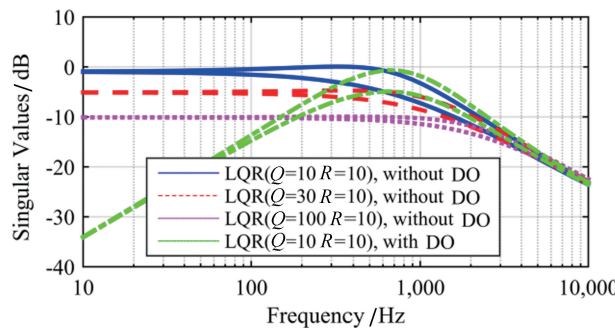


Figure 10 Singular Values of i_c/U_w for Disturbance Rejection analysis, with the rotor speed at $\omega_e = 300\text{Hz}$

As control constraint of tracking versus noise rejection exists in designing closed-loop control system, the Singular Values of $i_c/i_{e\xi}$ are also shown in Figure 11 for comparison. It's shown in the Figure that although sensor noise $i_{e\xi}$ is amplified a little bit by adding DO controller ($Q = 10$, $R = 10$), the magnitude over the high frequency range ($\geq 2\text{kHz}$), which is of interests for sensor noise, can be suppressed compared with increasing the system open-loop gain by selecting a higher Q index of the LQR ($Q = 30$ and 100 , $R = 10$).

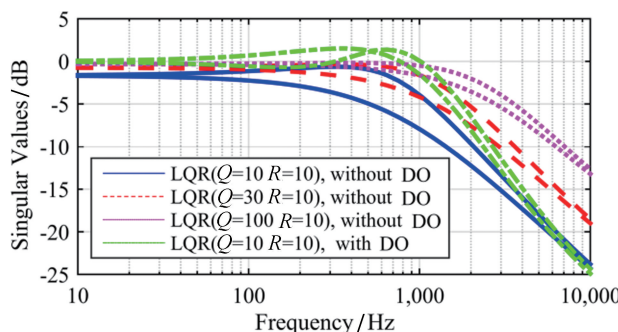


Figure 11 Singular Values of $i_c/i_{e\xi}$ for Noise Suppression analysis, with the rotor speed at $\omega_e = 300\text{Hz}$

3.2 Stability Performance Analysis

As stated above, the robust stability should be strictly guaranteed before the final implementation of the PHIL system. CT domain modeling and analysis methods have been widely used^[3,5,21], while [6] and [22] point out that the discretized modeling and impedance analysis method provides better prediction accuracy. As the MIMO EME system is modeled in discretized form as (18), method based on eigenvalue locations of DSS matrix is applied for reliable stability analysis here.

The open-loop EME system is stable only if eigenvalues of the system matrix A_{EME} in (18) lie inside the unit circle^[2]. The robustness of the stability is verified when operating speed of the EME system varies (see Figure 12) and modeling error of CN exists (see Figure 13). The EME system is robustly stable as the target operating speed/frequency of the motor is no more than 300Hz, and the modeling error coming from mass production of CN is no more than 35%, which is the same as [1].

Furthermore, the closed-loop EME testing system stability is also checked. Internal Mode Control (IMC)^[18] is widely used as the current control method for Motor Drives of the Electric Vehicle. So, IMC instead of PI controller used in [1] and [8], is selected as the control algorithm for MCU to analyze the overall EME testing system stability.

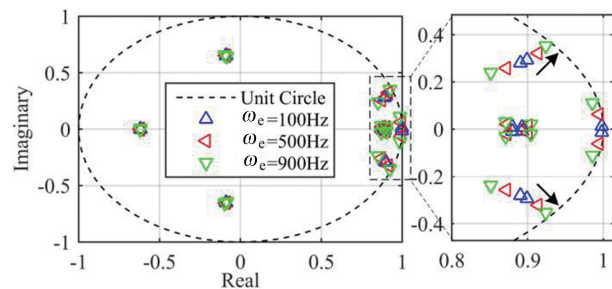


Figure 12 Eigenvalue migration of EME system when ω_e increases.

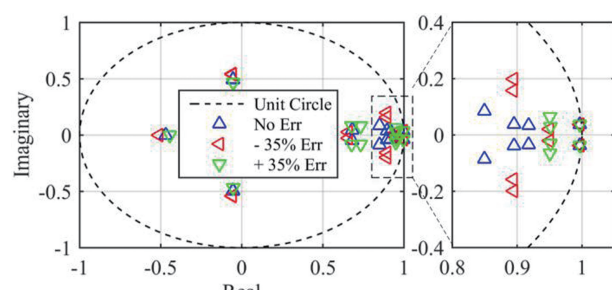


Figure 13 Eigenvalue migration of EME system with CN modeling error, with the rotor speed at $\omega_e = 300\text{Hz}$

It's of interest to check whether the stability of the system is sensitive to the ratios between the BW values of the MCU and the EME. Robust stability is guaranteed (see Figure 14) even when BW of DO of EME ($D_{OBW} = 20\text{Hz}$) is smaller than BW of IMC of MCU ($I_{mcBW} = 100\text{Hz}$), which is different from the analysis result of [8] in CT domain, who states that higher current-loop BW of EME compared with the DUT should be used to achieve stability. The main reason for the difference is that FF controller is used here to improve the dynamic and stability, which is also discussed in [5] in CT domain when emulating an SG using voltage type ITM.

Other factors that may affect the closed-loop EME testing system stability can also be analyzed by calculating the eigenvalues of the DSS system matrix, such as control delays, operating frequency, and modeling errors of the CN. Robust stability of the system is achieved by checking all these factors.

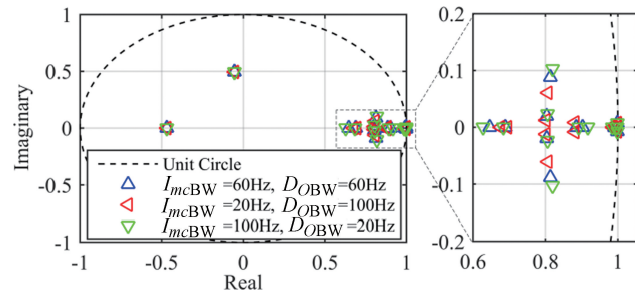


Figure 14 Eigenvalue migration of the closed-loop EME testing system with different ratios of BW values between IMC of MCU and DO of EME

4 EXPERIMENTAL RESULTS

The effectiveness of the proposed current control algorithm is verified on the prototype PHIL experimental setup shown in Figure 15. Power module based on parallel SiC MOSFET (Cree CAS120M12BM2) is implemented to increase the number of voltage levels of the phase voltage of EME. Other information about the experiment is shown in Table I.

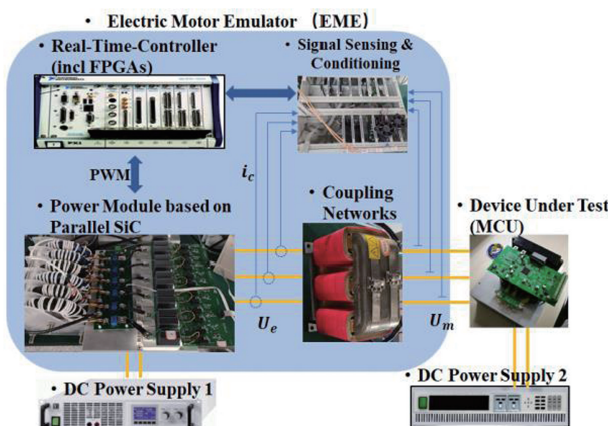


Figure 15 Experimental setup for EME testing system

TABLE I Information of Experimental Setup

MCU under test		Electric Motor Emulator (EME)	
DC Voltage	60V	DC Voltage	100V
Control Freq.	10kHz	Control Freq.	50kHz
Max. Current	50A (rms)	Max. Current	90A (rms)
Control Core	DSP	Control Core	FPGA
Topology	Two-level VSI	Topology	Multi-Level VSI

The tracking error between the real current i_e and the reference value i_m from the motor model in time domain is used here to assess the dynamic performance of the proposed control method quantitatively when MCU works at open-loop voltage mode. The desired Q Axis Current (see blue line of Figure 16a) tend to oscillate under step voltage output of MCU (see Figure 16b) since the system is under-damped (see Figure 3) when the rotor speed is high ($\omega_e = 300\text{Hz}$), and FF control alone can provide a relatively good tracking performance if no modeling error exists (see red line of Figure 16a), but tracking error deteriorates greatly when parameter error (35%) exists of the reference CN model [see green line and purple line of Figure 16a]. Voltage fluctuations/harmonics (6th order of ω_e) caused by dead-time effect of MCU^[23] are also captured (see Figure 16b) as the voltage sampling rate of EME system is 10MHz, which is much higher than that of the MCU.

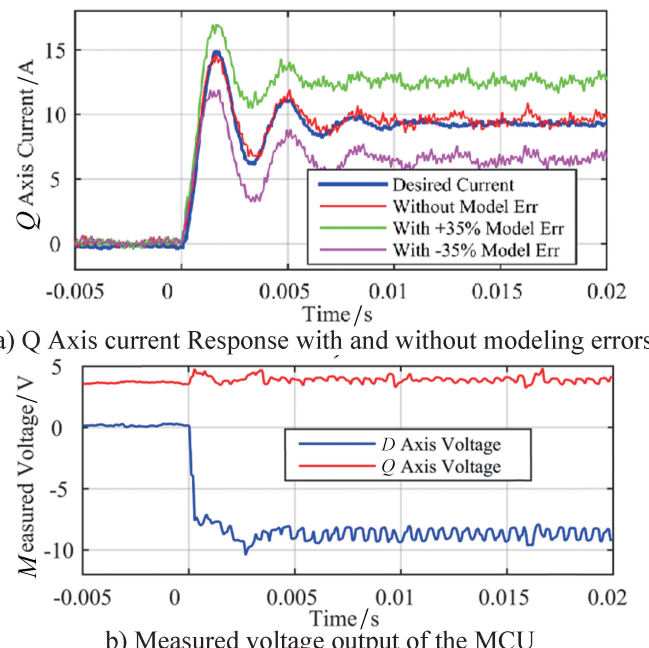
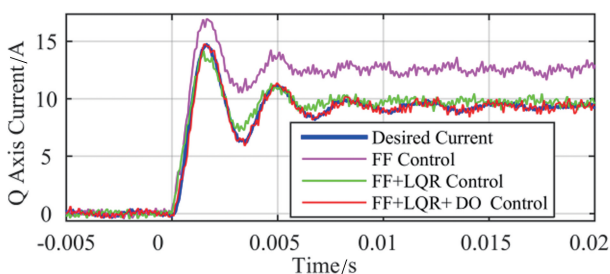
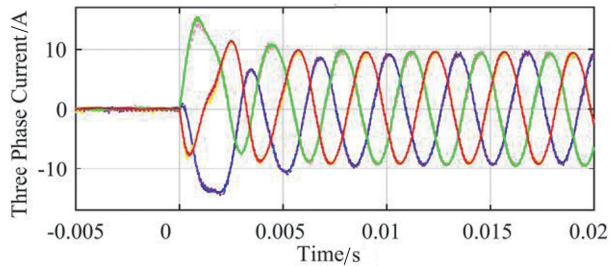


Figure 16 Current response of the EME system under step voltage input with only FF control when $\omega_e = 300\text{Hz}$

Tracking performance of the Q Axis current can be further improved by adding the state-feedback control (LQR) method to the Feedforward control when modeling error exists (see green and purple line of Figure 17a), but tracking error persists since



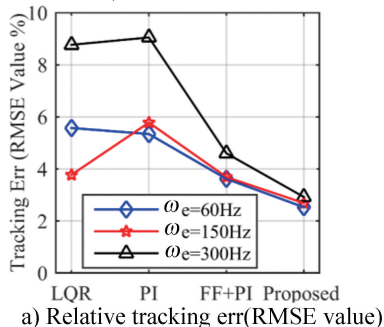
a) Q AxisCurrent response of different control method



b) Three phase current tracking performance when DO is adopted

Figure 17 Current response of the EME system with 35% modeling error when $\omega_e = 300\text{Hz}$

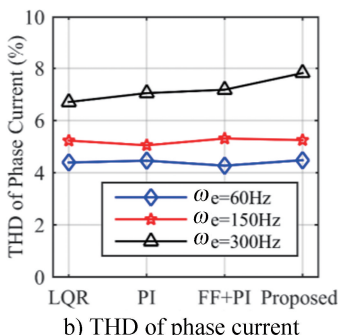
the steady state error cannot be eliminated (as analyzed in Section IV). As a contrast, the dynamic and steady state tracking error is almost fully removed by using the proposed control algorithm, in which DO is added (see red line of Figure 17a). Besides, the dynamic tracking results of the real three-phase currents to the desired values are also shown in Figure 17b, validating the effectiveness of the proposed control algorithm on emulating the ac power flow accurately.



a) Relative tracking err(RMSE value)

Three other types of the control algorithm (state-feedback control^[15], PI control^[1] and FF together with PI (FF+PI) control^[5]) are carried out to further compare the robustness with the proposed algorithm when 35% modeling error exists. The same design goal of BW is used for the other three types of control algorithm to make the comparison reasonable. It can be seen in Figure 18a that the proposed control algorithm can provide the lowest current tracking root-mean-square error (RMSE) value (around 3% of the desired current) compared with others at all operating speeds, i.e., 60Hz, 150Hz and 300Hz. Although FF + PI control algorithm can suppress the tracking error at low speed (less than 4% at 60Hz and 150Hz), the error increases as the operating speed goes up (4.5% at 300Hz). The total harmonic distortion (THD) value of the phase current when adopting the proposed algorithm is kept at the same level as others (see Figure 18b) at all speeds, though it may deteriorate a little bit (7.8% of the proposed algorithm compared with 7.2% of FF+PI) when speed increases to 300Hz.

The closed-loop control performance of the EME testing system is shown in Figure 19, current control based on IMC^[17] is used in MCU, and two values of $I_{mc,BW}$ (BW of IMC algorithm), i.e., 100 and 300rad/s, are set to compare the dynamic responses of the system. The oscillation suppression effect by using IMC in MCU is emulated, and the response time is about $t_r = \ln 9 / I_{mc,BW}$ ^[18], reflecting an accurate emulation effect of the EME system by using the proposed current control algorithm.



b) THD of phase current

Figure 18 Control Performance comparison between different control algorithms when 35% modeling error exists at different speed

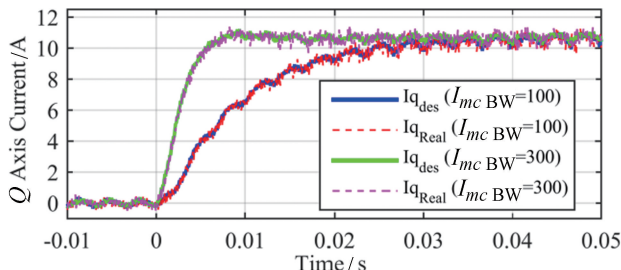


Figure 19 Current response of the closed-loop EME testing system, IMC is used as the current control algorithm for MCU

5 CONCLUSION

PHIL simulation is not plug and play^[4] considering accuracy and stability, especially for the case of EME testing system, which is more complex and demanding for robustness. A DO is developed, together with the FF controller and state feedback controller to form the proposed robust current control algorithm. The proposed algorithm brings the advantage that the system TFP competence is improved when operating speed varies and modeling error exists, since the unmodeled dynamics and/or disturbances of the system are estimated and compensated by the DO. Furthermore, the control goal of accuracy is derived based on Singular Value analysis in frequency domain of the target motor model, and the

stability is guaranteed by checking eigenvalues of the discretized motor model, open-loop EME system and closed-loop EME testing system step-by-step.

The robust effectiveness of the proposed control algorithm is validated through experiment by emulating a PMSM, showing its superiority in tracking performance at all operating speeds over the existing current control algorithm when 35% modeling error exists, and the THD value of phase current is kept at the same level. The proposed control algorithm and its analysis process can also be easily duplicated on other types of the PHIL system, considering its model-based attribute and the generalized discretized control law.

REFERENCES

- [1] LENTIJO S, D' ARCO S, MONTI A. Comparing the dynamic performances of power hardware-in-the-loop interfaces [J]. IEEE Transactions on Industrial Electronics, 2009, 57 (4): 1195-1207.
- [2] AYASUN S, FISCHL R, VALLIEU S, et al. Modeling and stability analysis of a simulation-stimulation interface for hardware-in-the-loop applications [J]. Simulation Modelling Practice and Theory, 2007, 15 (6): 734-746.
- [3] GUILLO-SANSANO E, SYED M H, ROSCOE A J, et al. Characterization of time delay in power hardware in the loop setups [J]. IEEE Transactions on Industrial Electronics, 2020, 68 (3): 2703-2713.
- [4] REN W, STEURER M, BALDWIN T L. Improve the stability and the accuracy of power hardware-in-the-loop simulation by selecting appropriate interface algorithms [J]. IEEE Transactions on Industry Applications, 2008, 44 (4): 1286-1294.
- [5] YANG L, WANG J, MA Y, et al. Three-phase power converter-based real-time synchronous generator emulation [J]. IEEE Transactions on Power Electronics, 2016, 32 (2): 1651-1665.
- [6] UPAMANYU K, NARAYANAN G. Improved accuracy, modeling, and stability analysis of power-hardware-in-loop simulation with open-loop inverter as power amplifier [J]. IEEE Transactions on Industrial Electronics, 2019, 67 (1): 369-378.
- [7] UEBENER S, BÖCKER J. Application of an e-machine emulator for power converter tests in the development of electric drives [C]. European Electric Vehicle Congress (EEVC). 2012: 1-9.
- [8] AMITKUMAR K S, KAARTHIK R S, PILLAY P. A versatile power-hardware-in-the-loop-based emulator for rapid testing of transportation electric drives [J]. IEEE transactions on transportation electrification, 2018, 4 (4): 901-911.
- [9] SCHMITT A, RICHTER J, BRAUN M, et al. Power hardware-in-the-loop emulation of permanent magnet synchronous machines with nonlinear magnetics-concept & verification [C]//PCIM Europe 2016; International Exhibition and Conference for Power Electronics, Intelligent Motion, Renewable Energy and Energy Management. Offenbach: VDE, 2016: 1-8.
- [10] LIEBIG S, SCHMITT A, HAMMERER H. High-dynamic high-power e-motor emulator for power electronic testing [C]//PCIM Europe 2018; International Exhibition and Conference for Power Electronics, Intelligent Motion, Renewable Energy and Energy Management. Offenbach: VDE, 2018: 1-5.
- [11] ZOU X, XIAO X, HE P, et al. Permanent magnet synchronous machine emulation based on power hardware-in-the-loop simulation [C]//2019 IEEE International Electric Machines & Drives Conference (IEMDC). Piscataway, NJ: IEEE, 2019: 248-253.
- [12] SLATER H J, ATKINSON D J, JACK A G. Real-time emulation for power equipment development. Part 2: The virtual machine [J]. IEE Proceedings-Electric Power Applications, 1998, 145 (3): 153-158.
- [13] GRUBIC S, AMLANG B, SCHUMACHER W, et al. A high-performance electronic hardware-in-the-loop drive-load simulation using a linear inverter (LinVerter) [J]. IEEE Transactions on Industrial Electronics, 2009, 57 (4): 1208-1216.
- [14] MONTI A, D' ARCO S, WORK Y, et al. A virtual testing facility for elevator and escalator systems [C]//2007 IEEE Power Electronics Specialists Conference. Piscataway, NJ: IEEE, 2007: 820-825.
- [15] RAO Y S, CHANDORKAR M C. Real-time electrical load emulator using optimal feedback control technique [J]. IEEE Transactions on Industrial Electronics, 2009, 57 (4): 1217-1225.
- [16] MEJIA-BARRON A, Valtierra-Rodriguez M, Amezquita-Sanchez J P, et al. A power hardware-in-the-loop scheme for load emulation applications [C]//2018 IEEE Inter-

- national Autumn Meeting on Power, Electronics and Computing (ROPEC). Piscataway, NJ: IEEE, 2018: 1-6.
- [17] LI Q, WANG D, LIN J, et al. Improving Dynamic Accuracy of the Electric Motor Emulator at High Speed via MIMO Design Method [J]. *IEEE Transactions on Power Electronics*, 2022, 37 (12): 14395-14407.
- [18] HARNEFORS L, NEE H P. Model-based current control of AC machines using the internal model control method [J]. *IEEE Transactions on Industry Applications*, 1998, 34 (1): 133-141.
- [19] KRAUSE P C, WASYNCZUK O, SUDHOFF S D, et al. Analysis of electric machinery and drive systems [M]. Hoboken: John Wiley & Sons, 2013.
- [20] CHEN W H, YANG J, GUO L, et al. Disturbance-ob-
- server-based control and related methods-An overview [J]. *IEEE Transactions on industrial electronics*, 2015, 63 (2): 1083-1095.
- [21] LAUSS G, STRUNZ K. Multirate partitioning interface for enhanced stability of power hardware-in-the-loop real-time simulation [J]. *IEEE Transactions on Industrial Electronics*, 2018, 66 (1): 595-605.
- [22] TREMBLAY O, FORTIN-BLANCHETTE H, GAGNON R, et al. Contribution to stability analysis of power hardware-in-the-loop simulators [J]. *IET Generation, Transmission & Distribution*, 2017, 11 (12): 3073-3079.
- [23] DAFANG W, BOWEN Y, CHENG Z, et al. A feedback-type phase voltage compensation strategy based on phase current reconstruction for ACIM drives [J]. *IEEE Transactions on Power Electronics*, 2013, 29 (9): 5031-5043.